Dispersion-corrected density functional theory comparison of hydrogen adsorption on boron-nitride and carbon nanotubes

Sridevi Krishnan, Rajasekarakumar Vadapoo, Kevin E. Riley, and Julian P. Velev

Phys. Rev. B **84**, 165408 — Published 6 October 2011

DOI: 10.1103/PhysRevB.84.165408

Dispersion-corrected density functional theory comparison of hydrogen adsorption on boron-nitride and carbon nanotubes

Sridevi Krishnan,[1] Rajasekarakumar Vadapoo,[1] Kevin E. Riley,[2,†] and Julian P. Velev[1,†]

[1] *Department of Physics, Institute for Functional Nanomaterials, University of Puerto Rico, San Juan, PR 00931, USA*
[2] *Institute of Organic Chemistry and Biochemistry, Czech Academy of Sciences, Prague, 16610, Czech Republic*

One of the main challenges for the future hydrogen economy is finding a safe and efficient way to store hydrogen. Materials with large surface areas, like carbon nanotubes and their analogues boron-nitride nanotubes, are being studied as potential candidates for this purpose. We perform density functional theory (DFT) and dispersion-corrected DFT (DFT-D) calculations of the adsorption of molecular hydrogen on graphene and boron-nitride sheets and compare against Møller-Plesset perturbation theory (MP2 and MP2.5). Our results indicate that DFT underestimates the binding energies while DFT-D gives a very good agreement with the higher order theory. Within DFT-D we show that the binding energy of molecular hydrogen to the outer walls of carbon nanotubes is more than 40% larger compared to boron-nitride nanotubes.

I. Introduction

The negative long-term environmental and economic impact of burning fossil fuels for energy will ultimately necessitate the transition to renewable energy sources. Although molecular hydrogen is generally recognized as the best potential candidate for a clean and sustainable source of energy, [1] hydrogen production as a mass commodity presents a number of technical challenges.[2] A necessary step towards the achievement of a hydrogen-based energy economy is the development of safe and efficient hydrogen storage technology. The Department of Energy (DOE) proposed target for efficient storage materials is hydrogen adsorption of 9 wt% (weight %) by 2015[3] and the optimum binding energy is in the range between physisorption and chemisorption (0.2-0.5 eV).[4] Potential storage materials include materials with large surface area such as graphene and carbon nanotubes. [5] In that respect a large body of experimental literature exists on the adsorption of atomic and molecular hydrogen on to the surface and inner walls of carbon nanotubes (CNTs). [6 - 10] The adsorption energy of molecular hydrogen is in the physisorption range of about 50 meV for carbon surfaces.[11,12] More recently, boron-nitride nanotubes (BNNTs) have also been studied for their hydrogen storage capability. It was suggested that BNNTs would be better than CNTs for hydrogen storage owing to the partial ionic character of the BNNT surface.[4] There is promising experimental evidence for the hydrogen storage capacity of BNNTs. Pristine BNNTs have shown modest hydrogen uptake of up to 1.8 wt% which is due to relatively large weight per surface area.[13-15] Various methods have been proposed to increase the surface area of the BNNTs and thus increase the hydrogen uptake.[13,14,16-18]

The theoretical work has been largely centered on the adsorption of atomic and molecular hydrogen on to the surface and inner walls of CNTs.[19 - 25] The binding energies for atomic hydrogen chemisorptions are in the order of 1eV,[19] which is higher than the target. On the contrary the physisorption of molecular hydrogen is an order of magnitude lower than the target. Using a force-field approach the binding energy of external molecular hydrogen adsorption of 20 meV and internal binding energy of 40 meV is reported for CNT (9,9).[22] Physisorption of molecular H_2 on the surface of zigzag CNT (10,0) was found to be 34 meV at about 3.44 Å from the CNT surface.[23] A maximum binding energy of 70 meV has been reported for H_2 molecule adsorbed at the outer walls of armchair CNTs using density functional theory (DFT).[19] When DFT with a Lennard-Jones dispersion

correction scheme for Van der Waals interactions was employed, an external binding energy of 61 meV and an internal binding energy of 220 meV have been reported for CNTs in 6-7 Å in diameter.[24] Metal doping, such as Ti[26] or Ca,[27] on the surface of CNTs was calculated within DFT to increase on average the binding energy to 0.2-0.3 eV per H_2 and also increases the uptake at high Ti coverage.

There are already a number of studies on atomic and molecular hydrogen adsorption on both pristine and doped BNNTs based on DFT. [4, 28-33] Similar to CNTs the binding energies for atomic H chemisorption on BNNTs are found to be an order of magnitude higher than the target: in the range of several eV.[28,30] Conversely the binding energy of molecular H_2 physisorption are typically an order of magnitude smaller than the target: 20-40 meV has been reported for armchair BNNT calculated using hybrid functionals;[28] 50 meV has been reported using ultrasoft pseudopotentials with a distance of approximately 3.5 Å from the surface of the nanotube.[33] A maximum of 90 meV for zigzag BNNT where hydrogen is about 3.1 Å above the surface has been reported.[28] Metal doping of BNNTs has been suggested to provide an intermediate regime, including Ti,[33] Pt,[34,35] and other transition metal[36] doping. Binding energies of hydrogen molecules close to the metal site of several tenths of one meV have been predicted.

Comparison of the hydrogen storage capacity of BNNTs and CNTs reports gives contradictory results: several studies indicate that the binding energy of molecular hydrogen on BNNTs is larger than on CNTs, possibly due to their heteropolar binding.[4,28,31] At the same time other studies show that both physisorption and chemisorption of hydrogen on BNNTs are less favorable energetically than on CNTs.[32] Moreover all calculations are performed within a DFT framework, which is known to poorly describe dispersion interactions.[37]

In this paper, we study the adsorption energy of molecular hydrogen on segments of BN and graphene sheets using a dispersion-corrected DFT method (DFT-D) and compare the results with those obtained using both second-order Møller-Plesset perturbation (MP2) methods and a scaled MP2.5 method. Then, hydrogen adsorption of CNTs and BNNTs are studied using DFT-D. The rationale is that dispersion interactions are the leading energy scale in this system, which standard DFT functionals fail to capture because of the long-range of the dispersive interaction. Accounting for the dispersion interactions within DFT-D we predict that CNTs are more suitable for hydrogen adsorption than BNNTs.

II. Structure and methods

The dispersion or Van der Waals (VdW) interaction is relatively weak, however, it can be the dominant interaction when chemical bonding and electrostatic forces are absent, which is the case in many systems of extreme importance including many biological structures. Thus the correct accounting of such interactions is crucial for accurate theoretical description of such systems. The VdW interaction arises completely from long-range electron correlations. The most commonly used DFT local and hybrid functionals ignore the non-local part of the exchange-correlation, thus failing to describe the VdW interaction.[37] Since this energy contribution is small, the error is negligible for the chemically bound compounds, which is the case for atomic hydrogen adsorption. However, H_2 is a chemically stable non-polar molecule and the VdW energy is the leading contribution in the physisorption of H_2 on CNTs and BNNTs.

Dispersion can be calculated using higher order chemical methods, however, at a great computational expense. [38] Recently, DFT-D functionals were developed in which the VdW interaction is included semi-empirically (for review see Refs. 39,40). The total energy is $E_{\text{DFT-D}} = E_{\text{DFT}} + E_{\text{DISP}}$ where E_{DFT} is the usual self-consistent Kohn-Sham energy and E_{DISP} is an empirical dispersion correction given by [41,42]

$$E_{\text{DISP}} = -\frac{1}{2}\sum_{i,j} C_{6ij} \sum_{\boldsymbol{R}} \frac{f_{\text{damp}}\left(\left|\boldsymbol{r}_{ij} + \boldsymbol{R}\right|\right)}{\left|\boldsymbol{r}_{ij} + \boldsymbol{R}\right|^6}$$

where $\boldsymbol{r}_{ij}$ is the interatomic distance vector, $\boldsymbol{R}$ are the lattice vectors, and f_{damp} is a damping function. The coefficients are typically chosen by fitting to the energies of a representative set of 22 non-covalently bonded compounds (S22).[43] This correction has been implemented for gradient-corrected functionals

(GGAs) and the plane-wave (PW) pseudopotential formalism in the Quantum-Espresso package.[44]

Because of the semi-empirical nature of DFT-D we calibrate our calculations by comparing the binding energies of molecular hydrogen on graphene and boron-nitride (BN) sheets segments (Fig. 1) calculated using DFT, DFT-D, DFT-D3, MP2 and MP2.5. The system is non-periodic and the dangling bonds are hydrogen terminated. Then we use the DFT-D method on BNNTs and CNTs with both armchair (5,5) and zigzag (9,0) chirality which are of almost the same diameter and are in the experimentally synthesizable range. DFT and DFT-D calculations were carried in the Quantum Espresso (QE) package.[45] It is well-known that the the local density approximation (LDA) produces electronic densities more homogenous than the exact ones which leads to overestimation of the binding energies.[46] This problem is especially severe in the case of weakly bound systems including those involving dispersive interactions, including graphene.[24] At the same time, it is generally believed that for molecular systems GGA improves significantly binding energies and lengths and is therefore predominantly used in the literature. In this work we use the Perdew-Burke-Ernzerhof (PBE) functional[47] with ultrasoft pseudopotentials.[48] The plane wave energy cutoff is set to 50 Ry. Energy convergence of 10^{-8} Ry and a uniform $1 \times 1 \times 8$ k-point grid is used for the nanotubes and gamma point only for the sheets. Structural optimization was performed within both DFT and DFT-D until the Hellman-Feynman forces are converged to 10^{-3} Ry/au.

Reference calculations for H_2 complexes with the graphene sheets and BN sheets were carried out in the MOLPRO package within the MP2 and MP2.5 methods. The MP2.5 method is based on a mutual cancellation of errors between MP2 and MP3 calculations. MP2.5 has been shown to produce binding energy errors that are very close to those of much more expensive methods, such as CCSD(T)/CBS.[49-51] The MP2.5 binding energy is given as

$$\Delta E_{CBS}^{MP2.5} = \Delta E_{CBS}^{MP2} + x[\Delta E_{bas-x}^{MP3} - \Delta E_{bas-x}^{MP2}]$$

where traditionally *bas-x* is a medium basis set, such as aug-cc-pVDZ or cc-pVTZ. When these basis sets are used the scaling factor, x, is generally set to 0.5. In this work bas-x is represented by a smaller basis set, namely 6-31G*. For this basis set the scaling factor is set to 0.9, which generally yields results that are very similar to those obtained with the larger bases.[52] In this implementation of the MP2.5 method, MP2/CBS binding energy values were determined by extrapolation from the cc-pVDZ and cc-pVTZ basis sets. Each term in the MP2.5 calculations utilizes counterpoise corrections to account for basis set superposition error.

The DFT-D3 binding energy calculations were also carried out in MOLPRO using the BLYP functional along with the TZVPP basis set. The D3 empirical dispersion correction contains both R^{-6} and R^{-8} terms, which has been shown to improve the description of dispersion interactions.[53]

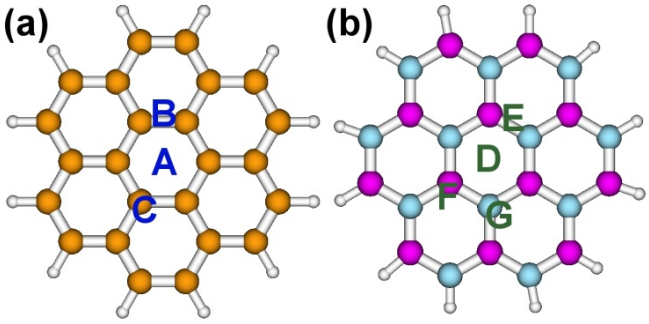

Figure 1: Hydrogen terminated segments of (a) graphene sheet showing the H_2 adsorption sites: A- hollow, B-bridge, C- top and (b) BN sheets showing the H_2 adsorption sites: D-hollow, E-bridge, F-B top, G-N top. Orange, magenta, cyan and white spheres represent C, B, N and H atoms respectively.

III. Results and discussion

The molecular hydrogen adsorption to segments of both graphene and boron-nitride sheets is studied using DFT, DFT-D(3), and MP2(.5). The binding energy of hydrogen molecule is calculated for several orientations of the molecule with respect to the graphene and boron-nitride sheets.

For graphene there are six possible configurations (Fig. 1a) – hollow (A), bridge (B) and top (C) positions with H_2 in vertical (V-hollow, V-bridge and V-top) and horizontal orientations (H-hollow, H-bridge and H-top). In the vertical orientation, the H_2 molecule is positioned perpendicular to the plane of the sheet and in the horizontal orientation parallel to the sheet. Fig. 2 shows the binding energies of H_2 to the

graphene at all of the above configurations. The comparison of the reported binding energies from Ref. 32 is also shown. We find that while standard DFT grossly underestimates the binding energy in all cases, the DFT-D shows binding energy very close to the values of MP2 and MP2.5. There is only slight orientation dependence with the hollow position being the most stable and the vertical orientation slightly more stable than the horizontal. Clearly DFT captures only a small part of the VdW interactions which is the predominant interaction between the sheets and the hydrogen molecule. It underestimates the binding energy 3-4 times and for some orientations even predicts repulsive interaction. The separation between the C sheet and the hydrogen molecule is relaxed separately within DFT and DFT-D. The average separation in the V- and H-configuration is 3.08 and 3.48Å in DFT respectively; 2.72 and 3.04Å in DFT-D. As expected the equilibrium separations in DFT-D are smaller by about 12%, because the interaction is more attractive.

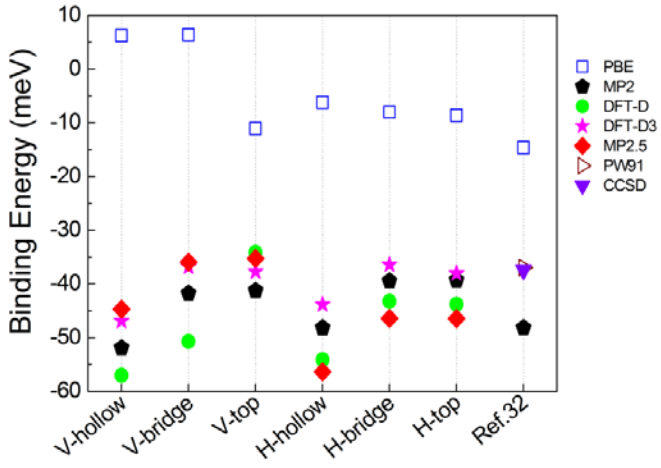

Figure 2: Binding energies of molecular hydrogen adsorption to segment of graphene sheet at different configurations using different methods. The preface V denotes that the H_2 is oriented perpendicular and H parallel to the graphene plane. The open symbols represent DFT methods while the closed ones represent higher order methods. In Ref. 32, the binding energy is reported for orientation V-hollow.

For boron-nitride sheets there are eight possible configurations (Fig. 1b) – hollow (D), bridge (E), top of boron (F) and top of nitrogen (G) in both vertical (V-hollow, V-bridge, V-B top and V-N top) and horizontal (H-hollow, H-bridge, H-B top and H-N top) orientations along with the reported values in the literature. Fig. 3 shows the comparison of the hydrogen molecule binding energy to the BN sheets in the above configurations. Here too standard DFT underestimates the binding energy; however, the difference is about 2 times. This is possibly due to the partially ionic character of the boron-nitride sheet for which DFT works better. On the other hand the standard DFT-D parameterization[42,44] of PBE in QE greatly overestimates the binding energy. The reason could be that the C_6 parameters are derived for compounds containing C and N (but not B) in higher coordination. To correct this we use a new and more accurate DFT-D parameterization which incorporates geometry- dependent information by using fractional coordination numbers to interpolate between dispersion coefficients of atoms in different chemical environments.[53] The new C_6 coefficients are 31.4436 a.u. for B and 15.5817 a.u. for N for coordination number close to 3 which is representative for the hexagonal sheet geometry. With this parameterization the binding energies from DFT-D are in much better agreement with MP2 and MP2.5 values (Fig. 3), although both DFT-D and DFT-D3 seem to overestimate the binding energy. The orientation dependence is even weaker with the different methods predicting different minima. The average separation in the V- and H-configuration is 3.06 and 3.36Å in DFT respectively; 2.79 and 3.13Å in DFT-D. Here the DFT overestimates the equilibrium distances by about 8% compared to DFT-D. The equilibrium separations for BN sheets are a bit larger than those for C sheets because the dispersive interaction is weaker.

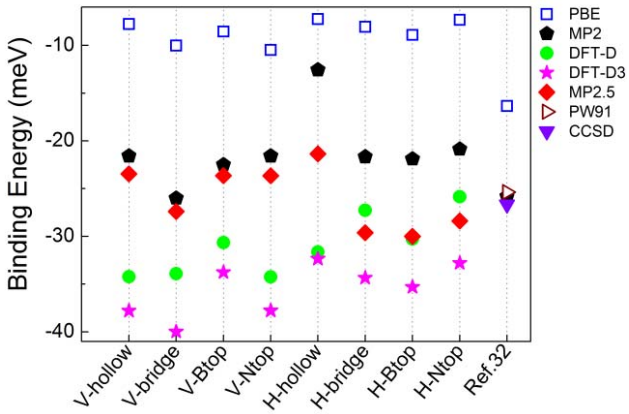

Figure 3: Binding energies of molecular hydrogen adsorption to segment of BN sheet at different configurations using different

methods. The preface V denotes that the H_2 is oriented perpendicular and H parallel to the sheet. The open symbols represent DFT methods while the closed ones represent higher order methods. In Ref. 32, the binding energy is reported for the orientation V-hollow.

Overall, a comparison of the DFT binding energies calculated here and elsewhere in the literature shows that the energies are underestimated; display large variability among the different implementations and functionals; and do not show any trend i.e. some show higher binding energy for graphene sheets while others for BN sheets. Higher order methods, on the other hand, predict much larger binding energies and show clearly that the graphene sheets have higher binding energy than the BN sheets. DFT-D agrees very well with the higher order methods and represents a systematic improvement over DFT (as opposed to coincidental agreement which was found for some DFT functionals) by providing the missing physics, namely the dispersive interactions. In addition, DFT-D predicts closer packing of the adsorbed hydrogen which would imply larger hydrogen uptake.

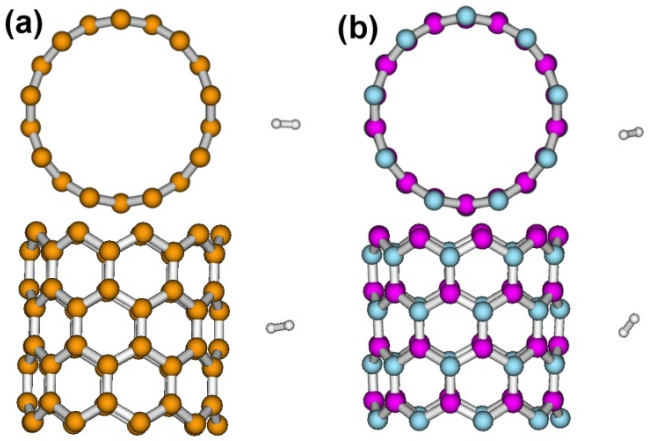

Figure 4: Optimized structures (top and side view) of a molecular hydrogen physisorbed at the outer wall of zigzag (a) CNT and (b) BNNT. The orange, magenta, cyan and white spheres represent C, B, N and H atoms respectively.

While it is possible to use higher order methods on small structures such as the graphene and BN sheet segments, these calculations become prohibitively expensive for realistic geometries. This is especially pronounced when geometry optimization is required. We found that DFT-D agrees very well with MP2.5 level of theory for these systems. Therefore, the real utility of DFT-D shows in study of larger structures such as the molecular hydrogen adsorption on the outer walls of the nanotubes which can be done with higher order methods' degree of accuracy but at the expense of a DFT calculation.

We consider armchair (5,5) and zigzag (9,0) C and BN nanotubes. These nanotubes have been studied in the literature and they are approximately the same diameter (~ 0.7 nm) within the experimentally synthesizable range. We optimized the position of a single H_2 molecule on all nanotubes. The optimized positions for zigzag (9,0) nanotubes of C and BN are shown in Fig. 4 . For armchair and zigzag CNTs we found the equilibrium separation to be 3.20 and 3.24Å in DFT respectively; 2.75 and 2.87Å in DFT-D. For armchair and zigzag BNNTs the equilibrium separations are 3.24 and 3.20Å in DFT; 2.97 and 2.91Å in DFT-D. The DFT overestimation is similar to the case of C and BN sheets.

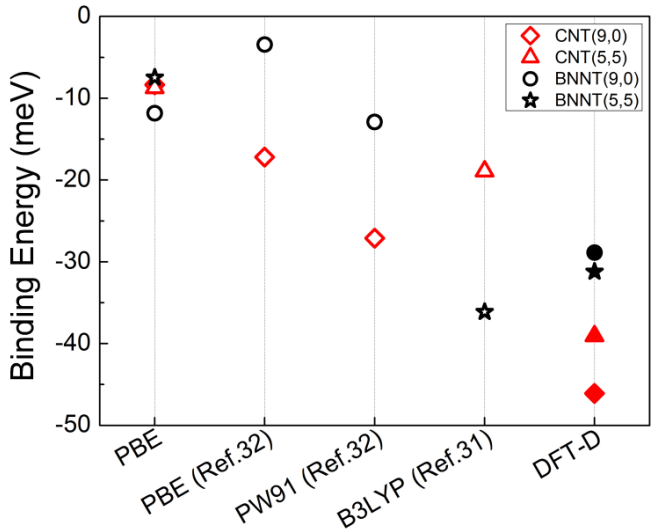

Figure 5: Comparison of binding energy of hydrogen adsorption to CNT and BNNT using different methods. The open symbols represent DFT methods while the closed ones represent higher order methods.

The chirality dependence of the binding energy of the nanotubes is almost negligible in case of DFT as shown in Fig. 5. Our DFT results show a very small increase in binding energy for the BNNT compared to the CNT which agrees with the results of Jhi *et al.*[28] and Mpourmpakis *et al.*[31] whereas results of Zhou *et al.*[32] show inclination towards CNT. DFT-D on the other hand clearly shows that the binding energy on BNNTs is smaller, which is consistent with the results for BN sheets. This could be explained by the fact that

even though the BN sheets are more ionic the H_2 molecule has a zero dipole moment. Therefore, the electrostatic interaction does not play a role and the interaction is purely dispersive. Due to the ionicity of BN sheets, more charge participates in fixed dipoles and less in induced dipoles, therefore the dispersive (London) interaction is weaker. The dispersive energy is approximated by[54]

$$E_{\mathrm{DISP}}^{A-B} = -\frac{3I_A I_B}{4(I_A + I_B)}\frac{\alpha_A \alpha_B}{r^6}$$

where I are the first ionization potentials and α are the polarizabilities of the molecules which in turn depend on the free charges. We observe that E_{DISP} is about a factor of two smaller for the stand-alone BN sheets compared to the C sheets therefore it must be that $\alpha_C > \alpha_{BN}$. From where it immediately follows that $E_{\mathrm{DISP}}^{C-H2} > E_{\mathrm{DISP}}^{BN-H2}$. The situation could be in reverse for molecules with non-zero dipole moment.

Our results, therefore, suggest that CNT are more appropriate for hydrogen storage applications. However, even though the binding energies within DFT-D are larger than the predicted values within DFT in this and previous studies they are still a lot smaller than required for practical applications.

IV. Conclusions

In summary, we have studied the molecular hydrogen binding to the graphene and boron-nitride sheet fragments using DFT, DFT-D(3), and MP2(.5). Our results indicate that DFT binding energies are underestimated and unreliable due to a well-known deficiency of the DFT functionals. At the same time DFT-D(3) seems to compensate very well for these deficiencies and shows very good agreement with MP2(.5) results for graphene and boron-nitride sheets. Using DFT-D we show that the molecular hydrogen binds stronger to carbon nanotubes compared to boron-nitride nanotubes. Since the equilibrium separation scales with the strength of the interaction DFT-D also predicts closer packing and potentially higher hydrogen uptake. Nevertheless, binding energies on pristine nanotubes are still well below the experimentally desirable range.

Acknowledgments

This work is supported by National Science Foundation (NSF) the Experimental Program to Stimulate Competitive Research (NSF grants EPS-1002410 and EPS-1010094). Computations were performed utilizing the Holland Computing Center at the University of Nebraska-Lincoln and the High Performance Computing facility at the University of Puerto Rico.

† Corresponding authors: JPV jvelev@gmail.com, KER kev.e.riley@gmail.com.

1. Department of Energy, A national vision of America's transition to a hydrogen economy (2002); Department of Energy, Hydrogen posture plan (2006).
2. V.S. Arunachlam & E.L. Fleischer, MRS Bulletin **33**, 265 (2008).
3. Department of Energy, Fuel Cell Technologies Program, www1.eere.energy.gov/hydrogenandfuelcells/mypp/
4. S.H. Jhi, Phys. Rev. B **74**, 155424 (2006).
5. L. Schlapbach & A. Zuttel, Nature **414**, 353-358 (2001).
6. D.S. Bethune, M.J. Heben, A.C. Dillon, K.M. Jones, T.A. Bekkedahl and C.H. Kiang, Nature **386**, 377-379 (1997).
7. A. Chambers, C. Park, R. T. K. Baker, N. M. Rodriguez, J. Phys. Chem. B **102**, 4253 (1998).
8. C. Liu, Y.Y. Fan, M. Liu, H.T. Cong, H.M. Cheng and M.S. Dresselhaus, Science **286**, 1127-1129 (1999).
9. H.M. Cheng, Q.H. Yang and C. Liu, Carbon **39**, 1447-1454, (2001).
10. M. Hirscher and M. Becher, J. Nanosci. Nanotechnol. **3**, 3-17 (2003).
11. G. Vidali, G. Ihm, H.-Y. Kim, and M.W. Cole, Surf. Sci. Rep. 12, 135 (1991).
12. H.G. Schimmel, G. Nijkamp, G.J. Kearley, A. Riveraa, K.P. de Jong, F.M. Mulder, Materials Science and Engineering B **108**, 124-129 (2004).
13. R. Ma, Y. Bando, H. Zhu, T. Sato, C. Xu and D. Wu, J. Am. Chem. Soc. **124**, 7672-7673 (2002).
14. C. Tang, Y. Bando, X. Ding, S. Qi and D. Golberg, J. Am. Chem. Soc. **124**, 14550-14551 (2002).
15. X. Chen, X.P. Gao, H. Zhang, Z. Zhou, W.K. Hu, G.L. Pan, H.Y. Zhu, T.Y. Yan and D.Y. Song, J. Phys. Chem. B **109**, 11525-11529 (2005).
16. R. Ma, Y. Bando, T. Sato, D. Golberg, H. Zhu, C. Xu and D. Wu, Appl. Phys. Lett. **81**, 5225-5227 (2002).
17. S.H. Lim, J. Luo , W. Ji & J. Lin, Catal. Today **120**, 346-350 (2007).
18. T. Terao, Y. Bando, M. Mitome, K. Kurashima, C.Y. Zhi, C.C. Tang & D. Golberg, Physica E **40**, 2551-2555 (2008).

19. J.S. Arellano, L.M. Molina, A. Rubio, M.J. López and J.A. Alonso, J. Chem. Phys. **117**, 2281 (2002)
20. S.M. Lee and Y.H. Lee, Appl. Phys. Lett. **76**, 287 (2000).
21. T. Yildirim and S. Ciraci, Phys. Rev. Lett. **94**, 175501 (2005).
22. M.K. Kostov, H. Cheng, A.C. Cooper, and G. P. Pez, Phys. Rev. Lett. **89**, 146105 (2002).
23. S.S. Han and H. M. Lee, Carbon **42**, 2169 (2004).
24. D. Henwood and J.D. Carey, Phys. Rev. B **75**, 245413 (2007).
25. W.J. Fan, R.Q. Zhang, B.K. Teo, B. Aradi and T. Frauenheim, Appl. Phys. Lett. **95,** 013116 (2009).
26. T. Yildirim and S. Ciraci, Phys. Rev. Lett. **94**, 175501 (2005).
27. H. Lee, J. Ihm, M. L. Cohen and S. G. Louie, Phys. Rev. B **80**, 115412 (2009).
28. S.H. Jhi and Y.K. Kwon, Phys. Rev. B **69**, 245407 (2004).
29. S.S. Han, S.H. Lee, J.K. Kang and H.M. Lee, Phys. Rev. B **72**, 113402 (2005).
30. X. Wu, J. Yang, J.G. Hou and Q. Zhu, J. Chem. Phys. **121**, 8481-8485 (2004).
31. G. Mpourmpakis and G.E. Froudakis, Catal. Today **120**, 341-345 (2007).
32. Z. Zhou, J. Zhao, Z. Chen, X.Gao, T. Yan, B.Wen and P. V. R. Schleyer, J. Phys. Chem. B **110**, 13363 (2006).
33. E. Durgun, Y.-R. Jang and S. Ciraci, Phys. Rev. B **76**, 073413 (2007).
34. X. Wu, J.L. Yang and X.C. Zeng, J. Chem. Phys. **125**, 044704 (2006).
35. X.M. Li, W.Q. Tian, X.-R. Huang, C.-C. Sun and L. Jiang, J. Mol. Struct.: Theochem **901,** 103-109 (2009).
36. S.A. Shevlina and Z.X. Guo, Appl. Phys. Lett. **89**, 153104 (2006).
37. T. Sato & H. Nakai, J. Chem. Phys. **131**, 224104, (2009).
38. G. Chalasinski, M.M. Szczesniak, Chem. Rev. **94**, 1723 (1994).
39. E.R. Johnson, I.D. Mackie and G.A. DiLabio, J. Phys. Org. Chem. **22**, 1127-1135 (2009).
40. M.E. Foster and K. Sohlberg, Phys. Chem. Chem. Phys. **12**, 307-322 (2010).
41. S. Grimme, J. Comput. Chem. **25**, 1463-1473 (2004).
42. S. Grimme, J. Comput. Chem. **27**, 1787-1799 (2006).
43. P. Jurečka, J. Šponer, J. Černy and P. Hobza, Phys. Chem. Chem. Phys. **8**, 1985-1993 (2006).
44. V. Barone, M. Casarin, D. Forrer, M. Pavone, M. Sambi and A. Vittadini, J. Comput. Chem. **30**, 934-939 (2009).
45. P. Giannozzi et al., J. Phys.: Cond. Matt. **21**, 395502 (2009).
46. J. Kohanoff, *Electronic Structure Calculations for Solids and Molecules: Theory and Computational Methods*, Cambridge University Press (July 24, 2006).
47. J.P. Perdew, K. Burke and M. Ernzerhof, Phys. Rev. Lett. **77**, 3865 (1996).
48. D. Vanderbilt, Phys. Rev. B **41**, 7892-7895 (1990).
49. M. Pitoňák, P. Neogrády, J. Černý, S. Grimme, P. Hobza, Chem. Phys. Chem. **10**, 282 (2009).
50. L. Gráfová, M. Pitoňák, J. Rezác and P. Hobza, J. Chem. Theory Comput. **6,** 2365 (2010).
51. K. E. Riley, M. Pitoňák , J. Černý and P. Hobza, J. Chem. Theory Comput. ***6,*** 66 (2010).
52. K. E. Riley, J. Řezač, P. Hobza, to be submitted.
53. S. Grimme, J. Antony, S. Ehrlich, and H. Krieg, J. Chem. Phys. **132**, 154104 (2010).
54. F. London, Z. Phys. **63**, 245 (1930).